3D Dynamic Simulation of Reinforced Concrete Seals for 120 psi Design Standard

R. Reddy Kallu, Graduate Research Assistant
Asmaa Yassien, Research Associate
Khaled Morsy, Research Associate
Syd S. Peng, Charles E. Lawall Chair of Mining Engineering
West Virginia University
Morgantown, WV

ABSTRACT

Prior to July 2007, the only accepted method by MSHA for evaluating the mine seal design and performance is the full-scale explosion tests conducted in the NIOSH's Lake Lynn Experimental Mine (LLEM) for deeming a seal design suitable for use in U.S. coal mines. Since the new regulations came into effect use of these conventional full-scale explosion tests for evaluating mine seals for the new elevated design standards may not be practicable. Generation of such high explosion pressures in experimental mines is dangerous and may cause permanent damage to the testing facilities. Further, they require significant amount of time, labor and money. Considering these factors, there is a need to develop scientific methods for evaluation of new seal designs and for understanding the dynamic seal response.

This paper tries to address the reinforced concrete (RC) seal design using the three dimensional finite element based explicit software ABAQUS. Full-scale explosion test data available from NIOSH's LLEM on 20 psi reinforced concrete seal is used for validating the numerical models. Further in this paper, based on the results from the validation models, a reinforced concrete seal is designed for 120 psi design standard for typical entry dimensions.

INTRODUCTION

Considering the practical difficulties involved in conducting the full-scale explosion tests for 120 psi seal designs, there is a need to develop new scientific methods and engineering practices for design, analysis and evaluation of mine seals. The current 120 psi seal design and evaluation practices are mostly based on simple analytical solutions. Applicability of these analytical solutions is every much limited because of the simple assumptions or limitations involved in the design process. So there is a need for developing a reliable methodology for addressing the seal design issues.

This paper mainly focuses on the use of numerical simulation techniques for design of reinforced concrete seals. Three dimensional finite-element based numerical simulation program, ABAQUS, is used as a tool for design of the 120 psi RC seals. This paper provides an in-depth analysis and understanding of how the reinforced concrete structures respond to the dynamic explosion pressure loading, also discusses the failure mechanism of the seal structures under these loading conditions. Full-scale explosion test results obtained from NIOSH's Lake Lynn Experimental Mine tests on reinforced structures are used for validation of the numerical models.

Factors Considered in RC Seal Design

A number of factors that affect the performance of the reinforced concrete seals are considered in this paper. Numerical models can be effectively used for evaluating these factors and help identifying the key influential parameters in the mine seal design. Factors considered in the current study include:

- Nature of explosion loading – The pressure-time curves proposed in the 30 CFR is used for design of reinforced concrete seals to comply with the regulatory requirements.
- Concrete constitutive behavior – Complete stress-strain curve in compression as well as in tension.
- Surrounding rock constitutive behavior - including roof, floor and coal ribs
- Interaction of the roof, floor and coal ribs with the seal structure
- Roof-to-floor convergence

ABAQUS Model: General

Figure 1 shows the general layout of the ABAQUS model. Two sets of vertical and horizontal rebars (grade 60 steel) are laid about 2.5 in. (cover distance) inside from both faces of the seal, in accordance with the guidelines suggested by the ACI (American Concrete Institute) for design of reinforced concrete structures.

After applying the appropriate initial and boundary conditions, interface properties, and constitutive behavior of materials the model is solved dynamically in two steps. In the first step, a very small amount of velocity is applied on the top face of the model to allow initialization of self weight of the structure. In the second step, explosion loading is applied on the inby face of the seal using the MSHA specified 120 psi pressure-time curve and the model is solved for the prescribed amount of time. A number of predefined monitoring points are selected in the model to record the history of seal's lateral displacements, seal response pressures and axial forces in the rebars.

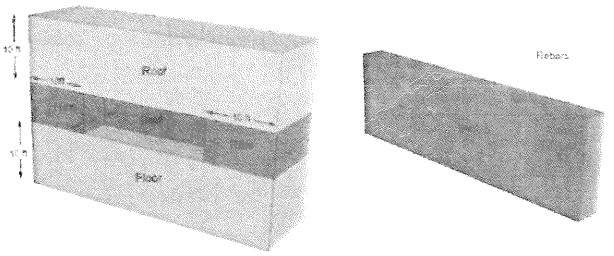

Figure 1. General layout of ABAQUS model.

MATERIAL MODELS

The immediate roof and floor rocks and coal are modeled using the extended Drucker-Prager model. Deformation prior to yielding is assumed to be linear elastic governed by the elastic parameters E and . The modified Drucker-Prager plasticity model in ABAQUS is intended for geological materials that exhibit pressure-dependent yield. The model uses non-associated flow in the shear failure region.

The reinforced steel rebar is assumed to behave as a bi-linear elastic-perfectly plastic material. A classical Von-Mises yield criterion with associated plastic flow is used in the modeling. The reinforced rebars are modeled as beam elements embedded in the host concrete/rock elements. These rebars are embedded into the roof and floor to a distance of 2 ft in the simulation models. The concrete and the internal steel rebars interaction is approximately considered in the modeling by tension stiffening of the concrete material model. The interface between the reinforced concrete seal and the surrounding rock is modeled using the bi-linear Coulomb friction model with zero cohesion. According to this model, sliding will occur if the magnitude of the shear stress along the interface reaches a critical value, τ_{max}, regardless of the magnitude of the contact pressure.

The geo-mechanical properties of the coal, immediate roof and floor rock, and reinforced steel rebars used in the models are given in Table 1.

Table 1. Geo-mechanical properties of rock, coal and steel.

Property	Rock	Coal	Steel
Young's Modulus (E), psi	3e+06	3e+05	2.9e+07
Poisson's ratio (υ)	0.19	0.35	0.28
Density, lbs/ ft^3	162.3	86.5	486
Friction angle	35	29	-
Dilation angle	0	0	-
Cohesion (psi)	370 psi	163 psi	-
Yield strength (psi)	-	-	60,000 psi

CEB & BARTH and WU CONCRETE MODEL

Non-linear behavior of concrete is simulated with a uniaxial stress-strain curve with strain softening and tension stiffening. The compressive part of concrete material model was initially developed by Comite European Du Beton (CEB) and has been verified by Barth and Wu (2006) by comparing the complete load-deflection relationships and ultimate capacities resulting from the finite element analysis of two simply supported composite girders and a 4-span continuous composite steel bridge with experimental data. Simply supported composite girder experimental tests were conducted by Mans (2001) at the University of Nebraska and the 4-span continuous composite steel bridge experimental test was reported by Burdette et al., (1971). Barth et al., (2006) used the finite element based software ABAQUS in their analysis.

The CEB compressive concrete model relates the stress-strain by the following equation which is a function of only one parameter (f'_c), yet it can accurately reflect the variation in response to different strengths that are observed in practice (Hognestad et al., 1955). However, it is noted that the compressive concrete constitutive law appears to have only minor effects on the overall results (ASCE, 1993; Cope and Rao, 1981).

$$f_c = \frac{0.85 f'_c (a - 206{,}000\,\varepsilon_c)\varepsilon_c}{1 + b\,\varepsilon_c}$$

where, $a = 6193.6(0.85 f_c + 1.015)^{-0.953}$
$b = 8074.1(0.85 f_c + 1.450)^{-1.085} - 850$
f_c = 28-day concrete compressive strength, ksi
ε_c = compressive strain in concrete

ABAQUS requires the inelastic material properties to be input in the form of true (Cauchy) stress (σ_{true}) and true (logarithmic) strain (ε_{true}), which can be calculated from the engineering stress (σ_{eng}) and engineering strain (ε_{eng}) using the following equations.

$$\sigma_{true} = \sigma_{eng}(1 + \varepsilon_{eng})$$

$$\varepsilon_{true} = \ln(1 + \varepsilon_{eng})$$

Using the above equations the stress-strain relationship in compression is plotted in figure 2. Based on data available in the literature (Wittry, 1993), a value of 0.0038 is assumed for the maximum compressive strain (ε_{cmax}). This value is typical American Concrete Institute (ACI) maximum compressive strain value and is thought to be conservative since higher values of crushing strain have been reported in physical tests (Wittry, 1993).

Barth and Wu, (2006) used a non-linear concrete tension model in the analysis, according to which the tensile stress increases linearly up to concrete cracking stress (f_t) and then unloads gradually. A parabolic curve passing through the concrete cracking point (f_t, ε_t) and concrete maximum strain point (ε_{tu}) is suggested for the gradual unloading portion by Barth and Wu (2006). Beyond the cracking stress concrete exhibits a significant tension stiffening behavior and the tensile load carrying capacity of the concrete decreases exponentially. The concrete and the internal steel rebars interaction is approximately considered by the tension stiffening

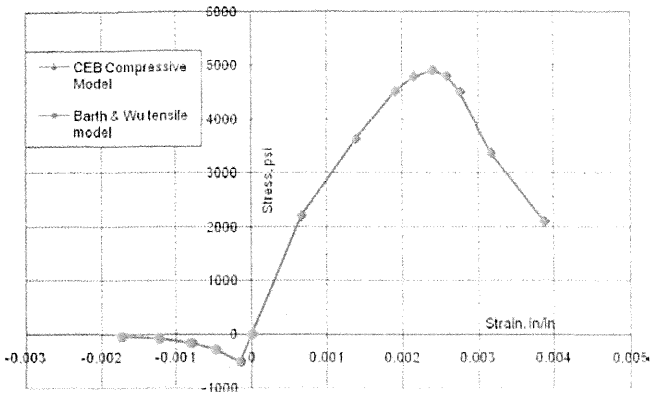

Figure 2. The stress-strain behavior of concrete in compression and tension.

behavior of the concrete. CEB & Barth et al., concrete model was used effectively used by Morsy et al., (2008) for simulating the non-linear behavior of concrete in the design of reinforced concrete seals.

Concrete Damaged Plasticity

The *Concrete Damage Plasticity* option in ABAQUS is used to define the yield function and flow potential. An isotropic damaged elasticity in combination with isotropic tensile and compressive plasticity is used in the *Concrete Damage* Plasticity model to better represent the inelastic behavior of concrete.

This concrete damaged plasticity model uses the yield function proposed by Lubliner et al., (1989) with the modifications suggested by Lee and Fenves (1998) to consider different evolution of strength characteristics under tension and compression. The evolution of the yield surface is defined by the hardening variables (equivalent tensile and compressive plastic strains).

The equivalent tensile and compressive plastic strain can be automatically calculated by ABAQUS using the *Concrete Tension Stiffening* and *Concrete Compression Hardening* options, and the tensile and compressive damages by using the *Concrete Tension Damage* and *Concrete Compression Damage* options, respectively.

Figure 3 shows the relationship between concrete damage and plastic strain for compression and tension (Barth and Wu, 2006). A damage variable close to 1.0 indicates complete failure of the material and, close to 0.0 indicates no-damage in the material.

VERIFICATION CASE

Although NIOSH engineers conducted extensive full-scale explosion tests in LLEM on mine seals constructed from various types of construction materials, there were only two tests that were conducted on seals constructed from concrete like materials with internal steel reinforcement that meet the reinforced concrete seal criteria (Zipf et al., 2008). These seals were tested for the old 20 psi design standard. Explosion overpressure was created by igniting a methane-air mixture in a confined area and monitored using pressure transducers. Lateral displacements on the outby side of the seal and at the center were monitored using LVDT's. The results from these full-scale explosion tests are used for validation of the predictions from the ABAQUS models. Results from simulation of one of these cases are presented in this paper.

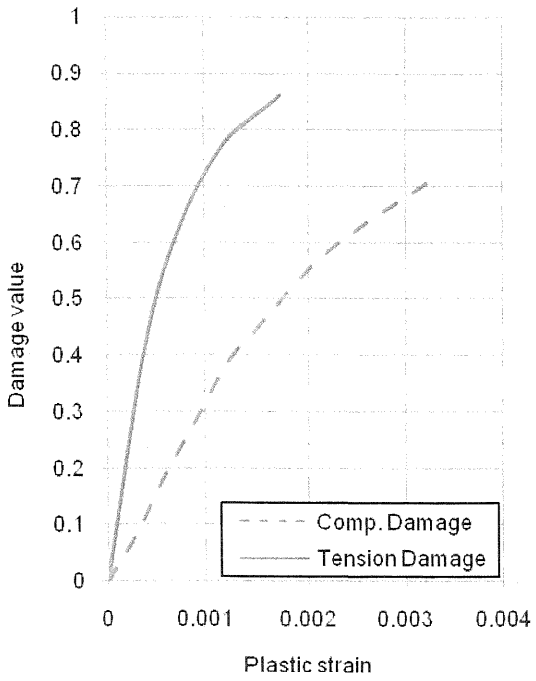

Figure 3. Relationship between concrete damage and plastic strain.

Insteel 3-D Seal: Construction details

The Insteel 3-D seal marketed by Precision Mine Repair, was constructed with concrete, steel reinforcement bars and wires. This seal survived the explosion test.

To construct the seal, vertical holes are drilled in two sets into the roof and floor to a depth of at least 12 in. and evenly-spaced across the entry on less than 2 ft centers. The vertical holes in the front and rear rows offset from each other laterally as shown in the figure 4. Three horizontal holes are also drilled into each rib to a depth of 12 in. on 2 ft centers, and, 3 ft long #8 steel rebar anchors are grouted into these vertical and horizontal holes. No hitching is made in to the roof and floor.

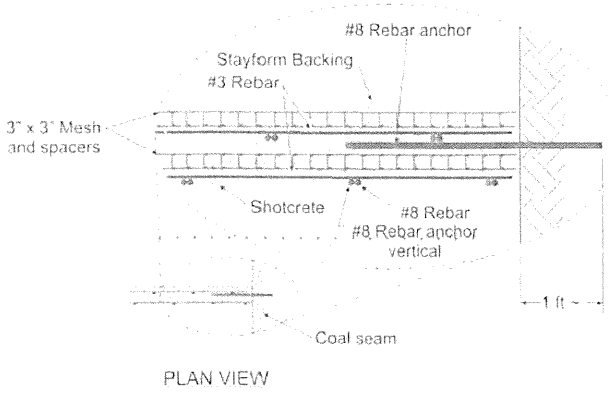

Figure 4. Schematic diagram of plan view of Insteel 3-D seal (Zipf et al., 2008).

The #8 reinforcement rebars are tied to the corresponding rebar anchors in the roof and the floor. Two sets of #3 horizontal steel reinforcement rebars are also laid from rib to rib and spaced less than 16 in. Insteel-3D panels are laid across the entry and tied to the front and rear rows of vertical rebars. Stayfoam backing was used on the inby side to hold the concrete in place. Shotcrete/ concrete (362 bags of Pak Mix Pro Line concrete mix or 25,340 lbs of dry mix) was applied to the entire structure to a total thickness of about 11.5 in.

The recorded history of explosion overpressure and the lateral displacements from the explosion test are presented in figure 5. The explosion pressure reached a maximum of value of 57 psi in just 0.1 sec and the lateral displacements reached about 0.075 in.

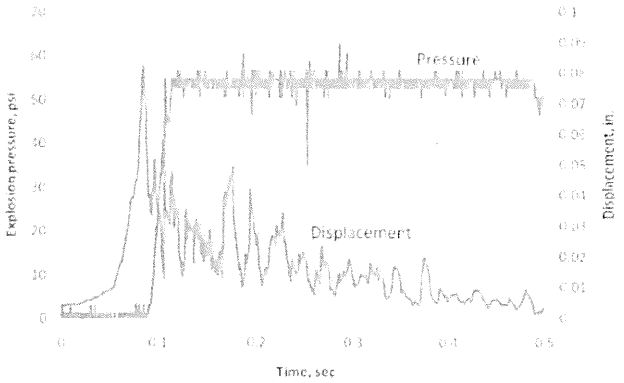

Figure 5. Recorded history of explosion overpressure and seal displacement.

ABAQUS Model: Verification Case

Using the seal construction details described in the previous section finite element based ABAQUS model was constructed. The exact pressure-time curve (figure 5) recorded in the full-scale explosion test was used for applying the explosion loading to the seal in the model. The CEB & Barth et al., concrete constitutive model discussed earlier in this paper was used for simulating the non-linear behavior of the concrete.

History of lateral displacement at the center of the seal on the outby face predicted by the model and the measured displacements from LVDT are plotted in the figure 6. The predicted displacements from the model and the measured displacements match very well with some exceptions. The rise time of the lateral displacement matches very well with the measured rise time, but the magnitude of peak displacement predicted from the model is offset by about 0.02 in. from the measured value. Further, it can be observed from figure 6 that lateral displacements predicted by the model are fluctuating and dampening over time, but the measured displacements are almost steady at about 0.08 in. This is because of the reason that the LVDT used in the measurement was not spring loaded. Figure 7 shows the contour of lateral displacements in the seal and in the steel rebars at 0.125 sec time.

Field observations from the explosion test documented that the seal has survived the explosion with very little damage. The ABAQUS model also predicts similar results. Figure 8 shows the

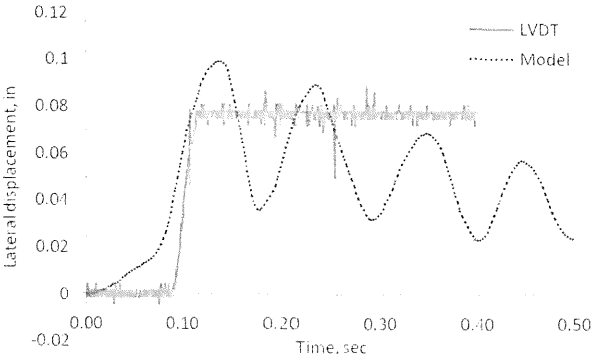

Figure 6. Predicted and measured lateral displacement-time curves.

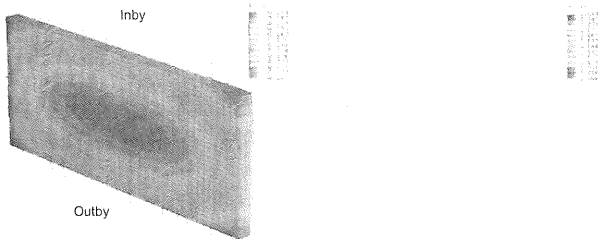

Figure 7. Lateral displacement contours (in seal and rebars) at 0.125 sec.

damage contours in the seal at 0.125 sec. A small horizontal tensile damage crack extending to about half the thickness of the seal is observed at mid height of the seal. The volume weighted average damage factor is calculated to be 0.01485 for this seal. The rebars in the seal show no signs of yielding.

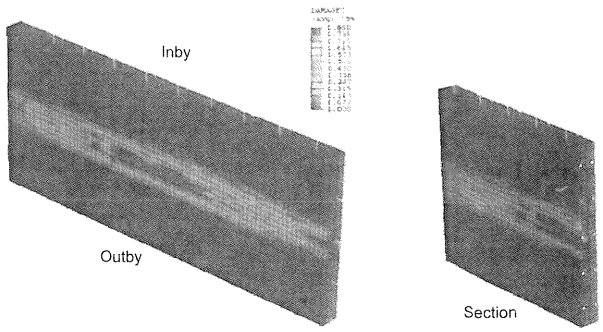

Figure 8. Damage contours in the seal at 0.125 sec.

The CEB and Barth et al., concrete model used in the ABAQUS verification model predicted very close results as compared to the measured experimental results. This verification case added some confidence to the modeling technique used in this paper.

DESIGN OF REINFORCED CONCRETE SEAL

The primary aim of this study is to understand the RC seal response to the dynamic explosion loading and the seal failure mechanism under these loading conditions. A number of finite element seal models were constructed with the following parameters.

Entry dimensions (h x w): 6 ft x 20 ft
Vertical rebar size & spacing: #9 and 10 in.
Horizontal rebar size & spacing: #6 and 18 in.
Seal-rock/coal interface strength: 200 psi
Seal thickness: 12 in., 15 in., 18 in., 21 in., 24 in. and 30 in.

The seal thicknesses varied from 12 to 30 in. The models were subjected to 120 psi instantaneous explosion loading pressure lasting for 4 sec.

RC Seal Mechanical Response

Figure 9 shows the contour of axial forces in the vertical rebars for different seal thicknesses. In 12 in. thick seal, a very high level of tensile axial forces are developed in the rebars on the inby as well as on the outby side. At this seal thickness, the reinforced concrete material shows complete failure in tension and offers no bending/shear resistance to absorb the explosion pressure. With the increase in seal thickness beyond 12 in. the axial forces in the inby rebars turn to compressive but the axial forces in the outby rebars still remain in tension. The structural integrity of the reinforced concrete improves significantly with the increase in seal thickness by offering high internal bending and shear resistance to absorb and transfer the explosion loading pressure effectively to the surrounding rock.

The magnitude of the axial forces in the rebars at mid height i.e., tensile forces in the outby rebars and the compressive forces in the inby rebars, decreases significantly with increase in seal thickness from 15 to 30 in. At the same time, tensile forces in the outby and inby rebars near the roof and floor line increase significantly with increase in seal thickness from 15 to 30 in. Beyond 24 in. seal thickness, the axial forces are concentrated in the sections of the steel rebars near the roof and floor line. This indicates that the seal has reached sufficient thickness to provide maximum internal bending resistance to the applied explosion loading and able to transfer the stresses to the steel rebars near the roof and floor lines, and eventually to the surrounding rock. At higher thickness, seal behaves like a plug rather than just bending.

The schematic diagrams shown in figure 10 explain this phenomenon clearly. These diagrams show the amount of axial forces (in thousand lbs) developed in the central vertical rebar at the monitoring locations. The numbers shown in red indicate the magnitude of tensile forces and the numbers shown in blue/ parenthesis indicate the magnitude of compressive forces. The maximum axial forces developed in the steel rebars are well below the yield strength of the steel. Legend: RL – Roof Line, FL – Floor Line, T – Tensile, C – Compressive.

Figure 11 shows the history of lateral displacements on the outby side of the seal at mid height for different seal thickness. The the lateral displacement history in the 12 in. thick seal shows that the displacements are constantly increasing over time and reach a maximum value of about 1.2 in. over a period of 4 sec. This indicate

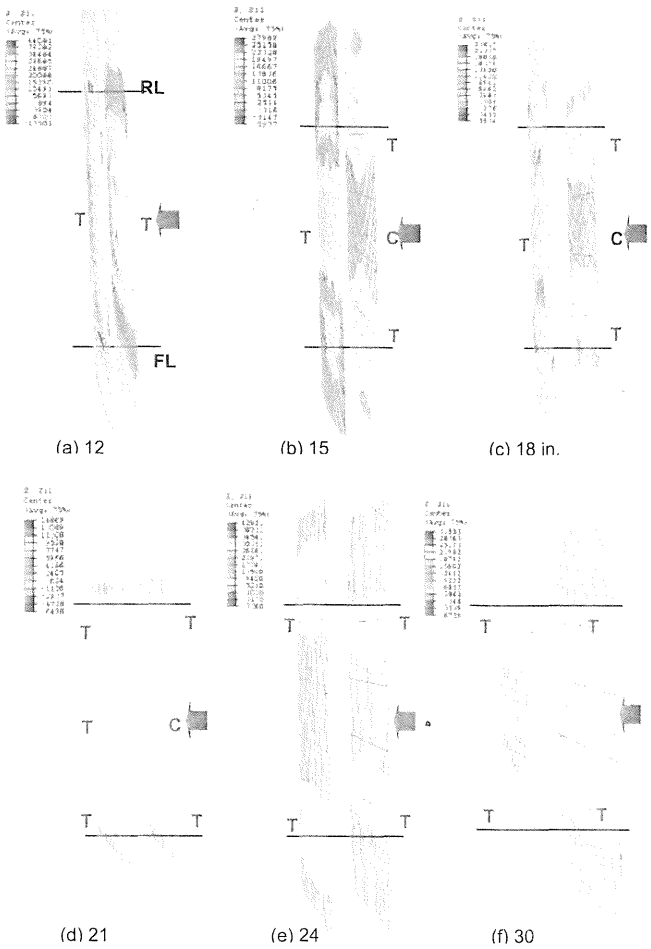

Figure 9. Axial forces in the rebars for seals with different thickness.

the continuous deformation of the seal under the applied explosion loading pressure. The magnitude of the lateral displacements reduces significantly with the increase in seal thickness from 12 to 21 in. thick, and very much stabilizes over time. Further increase in seal thickness to 24 in. and beyond actually increases the magnitude of the lateral displacements. This is mainly because of the change in the basic seal response to the explosion loading at higher seal thicknesses. The following paragraphs explans this particualr behavior of seal.

Figure 12 shows the plot of the maximum lateral dipslacements for different seal thickness measured at various locations in the seal. The displacements in the seal near the roof and floor are very much the same. The difference in the displacements at Outby_M and Outby_T/B decreases sharply with increasing in seal thcikness but once the seal has reached sufficient thickness the difference approaches near zero and remains constant with further increase in seal thickness. This indicate that at higher thickness seal behaves like a rigid body and tries to shear along the seal interfaces under the applied explosion loading. The seal in turn transfers the applied explosion loading to the surrounding rock through steel rebars and seal interfaces. This causes the sections of the rebars near the roof and floor lines to be subject to high tensile stresses.

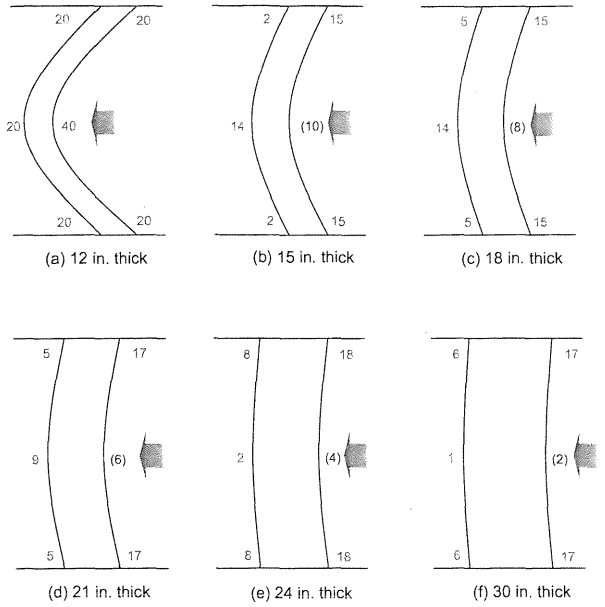

Figure 10. Schematic diagrams for axial forces (shown in thousand lbs) in the rebars.

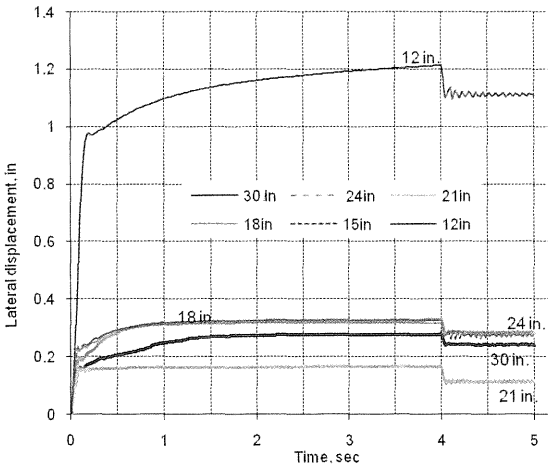

Figure 11. History of lateral displacements for different seals at outby_M.

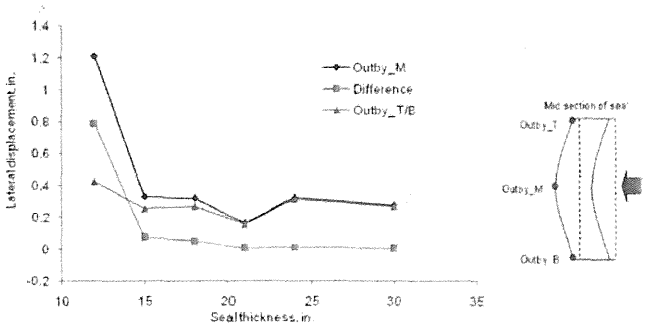

Figure 12. Maximum lateral displacement Vs seal thickness.

Figure 13 shows the damage contours in the concrete material on the outby face of the seals for different seal thicknesses. The red contour lines with damage values close to 1.0 indicate the tensile cracks on the outby surface of the seals. Under the applied explosion loading presssure, the 12 in. thick seal exhibits extensive damage with numerous horizontal and vertical tensile cracks on the outby surface of the seal. With an increase in seal thickness beyond 12 in. the extent of damage reduces significantly. There is some noticeable localized damage observed in the concrete along the rebar line near the roof and the floor. This localized damage is mainly because of the punching effect of the rebars on the concrete cover, which is about 2.5 in., and has a very little influence on the overall stability of the seal.

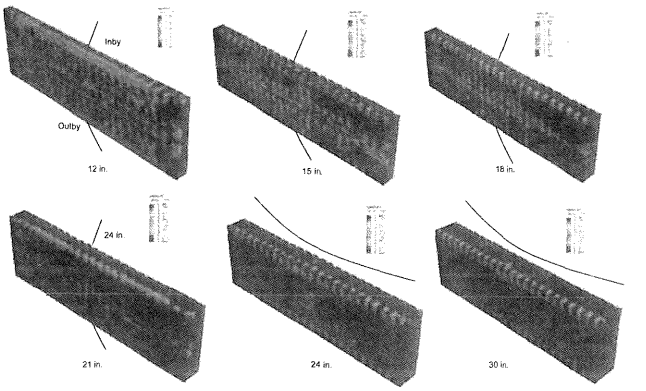

Figure 13. Damage contours in seals with different thickness.

The 15 in. thick seal shows some simple horizontal and vertical cracks on the outby face of the seal. An increase in seal thickness from 15 to 21 in. has reduced the concrete cracking from multiple cracks to a single horizontal crack running parallel to the seal on the outby face at mid height. Under the applied explosion loading the seal bends over its height, when it is sufficiently thin, and causes the horizontal tensile cracks develop on the surface of the seal. When the seal is sufficiently thick, 24 in. and beyond in this particular case, it bends over its length and develops vertical tensile cracks on the outby surface of the seal. The curved lines shown in figure 13 shows how the seal deforms in each case.

In either case, bending of the seal under the explosion loading causes the inby section of the seal to be subject to compressive stresses and the outby section of the seal to be subject to tensile stresses. Concrete being weaker in tension develops tensile cracks on the outby surface of the seal, whereas the inby surface of the seal shows no signs of damage. These tensile cracks extend only half way deep into the seal (Figure 14). Also notice in Figure 14 the development of shear failure surfaces originating from the top outby corner of the seal and extending deep into the seal. The extent of the shear failure is reduced significantly with increase in seal thickness to 21 in. and beyond.

It is important to recognize the fact that development of the cracks in normal concrete cannot be avoided unless otherwise the seal is highly overdesigned or constructed using the fiber reinforced concrete material. Simple cracking in the concrete does not necessarily indicate the complete failure of the seal. The primary purpose of installing the reinforced rebars close to the seal surface

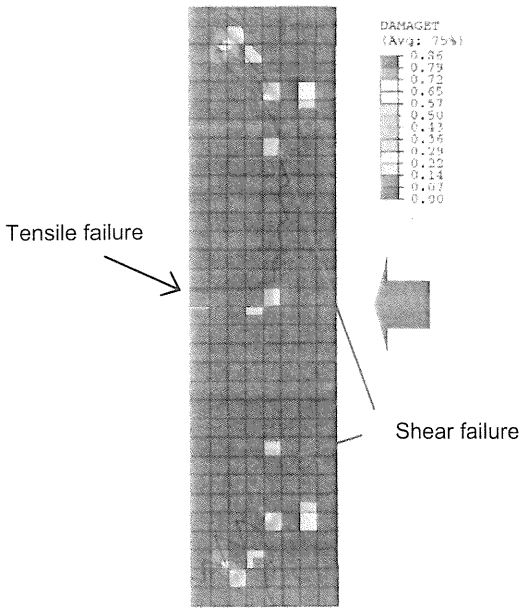

Figure 14. Damage contours in 18 in. thick seal (Mid-vertical section).

is to take care of the high tensile stresses that may develop near the surface of the seal in the event of an explosion.

Figure 15 shows the plot of weighted average damage factor (WADF) for different seal thicknesses. The WADF decreases sharply with increase in seal thickness to 21 in. and reaches a value of about 0.057. Further increase in seal thickness beyond 21 in. showed very little change in WADF. This WADF plot can be effectively used for determining the optimal thickness of a reinforced concrete seal for a given entry dimension.

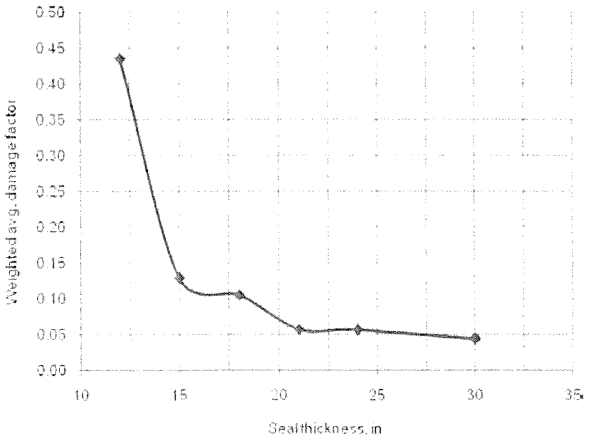

Figure 15. Weighted average damage factor (WADF) for different seal thickness.

CONCLUSION

Numerical modeling techniques can be effectively used as a tool for design of reinforced concrete seals. This paper provides better understanding of the reinforced concrete seal response to the explosion loading and the seal failure mechanism under dynamic loading conditions.

Concrete being weaker in tension develops tensile cracking on the outby surface of the seal. Simple tensile cracks on the outby surface of the seal not necessarily indicate the complete failure of the seal. Internal reinforced rebars takes care of the high tensile stresses that may develop near the surface of the seal in the event of an explosion. Further, the axial forces developed in the steel rebars are very much within the yield strength of the steel. Modeling results show that, when the seal is sufficiently thick, the tensile cracks developed on the surface of the seal extend only to half thickness of the seal and thus preventing the leakage of gases through cracks from the sealed-off areas. A combination of factors discussed in the paper including, weighted average damage factor, tensile cracking pattern, lateral displacements etc., can be effectively used for optimal design of reinforced concrete seals.

ACKNOWLEDGEMENT

This project was sponsored by CDC (NIOSH) – Mine Safety and Health through Contract No. 2007-N-09921.

REFERENCE

1. ACI 318-95, Building code requirements for structural concrete and commentary, American Concrete Institute.
2. ASCE (1993). State-of-the-Art Report on Finite Element Analysis of Reinforced Concrete, ASCE, New York, NY.
3. Barth, K. E., and H. Wu, (2006). Efficient nonlinear finite element modeling of slab on steel stinger bridges, Finite elements in analysis and design, Volume 42, No. 14, pp. 1304-1313.
4. Burdette, E.G., and Goodpasture, D. W., (1971). Final report in full scale bridge testing an evaluation of bridge design criteria, Department of Civil Engineering, the University of Tennessee, USA.
5. Cope, R. J., and Rao, P. V. (1981). "Non-Linear finite element strategies for bridge slabs." IABSE Colloquium, Delft University, Netherlands, pp. 273-288.
6. Hognestad, E., Hanson, N. W., and McHenry, D. (1955). "Concrete stress distribution in ultimate strength design." J. American Concrete Institute, 27(4), pp. 454-479.
7. Lee, J., and Fenves, G. L. (1998). "Plastic-damage model for cyclic loading of concrete structures." Journal of Engineering Mechanics, 124(8), pp. 892-900.
8. Lubliner, J., J. Oliver, S. Oller, and E. Oñate, (1989). "A plastic-damage model for concrete." International Journal of Solids and Structures, 25, pp. 299-329.
9. Mans, P.H., (2001). Full scale testing of composite plate girder constructed using 70-ksi high performance steel, M.S. Thesis, 2001, University of Nebraska-Lincholn, USA.
10. Morsy, M., A. Yassien, R. R. Kallu and S. S. Peng, (2008). Numerical simulation of reinforced concrete mine seal subjected to explosion loading, 27th International Ground Control Conference on Ground Control in Mining, July 2008, pp. 180-188.
11. Wittry, D. M. (1993). "An analytical study of the ductility of steel-concrete composite sections."M.S Thesis, the University of Texas at Austin, USA.
12. Zipf, R. K., E. S. Weiss, S. P. Harties, and M. J. Sapko, (2008). Compendium of Structural Testing Data of 20 psi Coal Mine Seals. Pittsburgh, PA: U.S. Department of Health and Human Services, National Institute for Occupational Safety and Health, IC in progress.

Proceedings

28th International Conference on Ground Control in Mining

Edited by

Syd S. Peng[1]
Thomas Barczak[3]
Chris Mark[3]
Steve Tadolini[2]
Gerry Finfinger[4]
Keith Heasley[1]
Yi Luo[1]

1. West Virginia University, Mining Engineering Department, Morgantown, WV
2. Minova Americas, Georgetown, KY
3. NIOSH-Pittsburgh Research Lab, Pittsburgh, PA
4. NIOSH, Pittsburgh, PA

July 28-30, 2009
Lakeview Scanticon Resort & Conference, Morgantown, WV, USA

ISBN 978-0-9789383-3-8